

Coherent optical manipulation of triplet-singlet states in coupled quantum dots

Hakan E. Türeci,¹ J. M. Taylor,² and A. Imamoglu¹

¹*Institute of Quantum Electronics, ETH-Zürich, CH-8093 Zürich, Switzerland*

²*Department of Physics, Massachusetts Institute of Technology, Cambridge, Massachusetts 02139, USA*

(Received 17 November 2006; revised manuscript received 29 March 2007; published 12 June 2007)

We show that spin-orbit coupling in a quantum dot molecule allows for coherent manipulation of two-electron spin states using Raman transitions. Such two-electron spin states defined by the singlet and triplet states of two exchange-coupled quantum dots can have favorable coherence properties. In addition, two of the four metastable ground states in this system can be used as auxiliary states that could facilitate implementation of tasks such as mapping of spin states to that of a single propagating photon. We find that even weak spin-orbit effects—manifesting themselves as slightly different g factors for the electron and the hole—would allow for the coherent Raman coupling of the singlet-triplet states. We also discuss the possibilities for implementing quantum optical techniques for spin preparation and manipulation.

DOI: [10.1103/PhysRevB.75.235313](https://doi.org/10.1103/PhysRevB.75.235313)

PACS number(s): 78.67.Hc, 03.67.Lx

I. INTRODUCTION

Over the past decade, semiconductor quantum optical systems, implemented in quantum wells and particularly quantum dots, have been paradigmatic for the exploration of novel quantum-mechanical effects in the solid state.¹ Potential applications as single-photon sources^{2,3} or as quantum bits for quantum information storage and processing⁴ have driven investigations of single quantum dots with ground states containing zero or a single electron charge. These systems bear marked resemblance to noble gas and alkali atoms. However, systems similar to alkaline-earth atoms (with two valence electrons) or homonuclear alkali molecules remain largely unexplored. Such systems typically have a more complex fine structure, leading to metastable spin states with useful decoherence properties⁵ and have well-established semiconductor realizations.^{6,7}

In this paper, we examine approaches for optically coupling the four metastable ground (spin) states of a two-electron double quantum dot system via optical Raman transitions. These states, split into a singlet and a triplet manifold, have demonstrated useful properties with respect to spin-related dephasing,^{8–10} as seen in recent experiments in electrically controlled double quantum dots.¹¹ Our approach for coupling singlet and triplet states via optical fields can lead to the integration of optical manipulation, measurement, and entanglement techniques with demonstrated approaches to controlling fine-structure states in electrical quantum dots.

While we focus on the case of zinc-blende (III-V) semiconductor quantum dots, we find that optical coupling of ground-state spins can be realized even with weak spin-orbit interaction, where a sufficient condition is that the electron and hole states have differing g factors; this is believed to be the case for small radius carbon nanotubes.¹² Thus, our approach for working with fine-structure states can find wide application in a variety of quantum dot systems.

II. COHERENT OPTICAL MANIPULATION OF COUPLED QUANTUM DOTS WITH STRONG SPIN-ORBIT EFFECTS

In this section, we develop an approach to coupling singlet and triplet fine-structure states of a double quantum dot

system via optical Raman transitions. We rely on the dramatic difference between exchange energies for two electrons on the same quantum dot and two electrons in separated quantum dots to provide a reliable means of using single spin selection rules to develop controlled, two-spin selection rules. We find that for doubly charged double quantum dots with spin-orbit coupling, such as zinc-blende semiconductor quantum dots, polarization- and energy-selective transitions between all fine-structure states are possible. This allows techniques, such as stimulated Raman adiabatic passage (STIRAP), to be used to initialize arbitrary superpositions of singlet and triplet spin states.

We consider here the optical transitions in a doubly charged coupled quantum dot (CQD), a situation that can, for instance, be realized with an asymmetric pair of stacked InAs quantum dots embedded in a Schottky-diode structure⁷ in an appropriate gate voltage regime. We assume that the left dot (L) is blueshifted with respect to the right dot (R) and that the lowest conduction level of the right dot is detuned by Δ with respect to the left one (see Fig. 1, inset). Higher orbital states can be neglected as the associated transitions are well separated in energy in the gate voltage regime of interest. For a range of gate voltages where the two dots contain a total of two electrons, by fine tuning the voltage, it is possible to convert between atomic and molecular orbital states,⁷ i.e., between charge states (0,2), (2,0), and (1,1). Labels (m,n) here refer to the number of electrons confined in the (left, right) dot. In the presence of finite interdot tunneling and in the regime where (1,1) is the lowest-energy charge configuration, the two resident electrons hybridize resulting in an energetically isolated singlet-triplet subspace where the effective degree of freedom is the total spin of the two electrons. This regime is denoted by II in Fig. 1 and in what follows, we will work in this regime.

In the (1,1) regime (II), the ground-state manifold is given by the states $|(1,1)S\rangle = \frac{1}{\sqrt{2}}(e_{L\uparrow}^\dagger e_{R\downarrow}^\dagger - e_{L\downarrow}^\dagger e_{R\uparrow}^\dagger)|0\rangle$, $|(1,1)T_0\rangle = \frac{1}{\sqrt{2}}(e_{L\uparrow}^\dagger e_{R\uparrow}^\dagger + e_{L\downarrow}^\dagger e_{R\downarrow}^\dagger)|0\rangle$, $|(1,1)T_+\rangle = e_{L\uparrow}^\dagger e_{R\uparrow}^\dagger|0\rangle$, and $|(1,1)T_-\rangle = e_{L\downarrow}^\dagger e_{R\downarrow}^\dagger|0\rangle$ with energies $E_{S_0} = \Delta + E_c^{LR} - \mathcal{J}$, $E_{T_0, T_\pm} = \Delta + E_c^{LR}$, where $\mathcal{J} \approx T_e^2/(E_C^{RR} - E_C^{LR})$. The typical energies for an InAs self-assembled quantum dot are given by $E_C^{LL} \approx E_C^{RR} = V_{LL,LL}^{ee} \approx 20$ meV, $E_C^{LR} = V_{LL,RR}^{ee} \approx 10$ meV, where $V_{ij,kl}^{ab}$

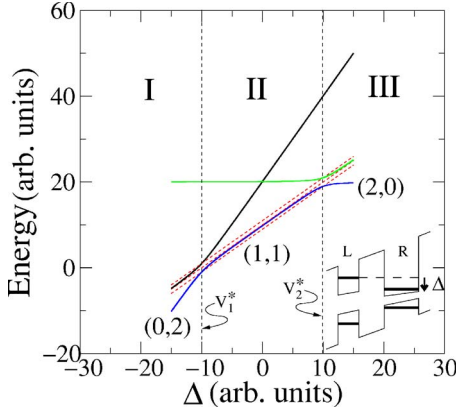


FIG. 1. (Color online) The energy-level structure of the coupled dot system as a function of the detuning Δ . The charge state of the ground state follows the sequence (0,2), (1,1), (2,0) from left to right. $\Delta = V_i^*$ ($i=1,2$) denote the anticrossing points at which the system undergoes a charge transition. The dashed lines show the triplet states $|(1,1)T_0\rangle$ and $|(1,1)T_{\pm}\rangle$. The ground state is always in the singlet configuration at low magnetic fields. In the inset, we show the single-particle level structure of the coupled quantum dots. The detuning $\Delta < 0$ for the configuration shown.

$= \int \int d\mathbf{r} d\mathbf{r}' \varphi_i^a(\mathbf{r}) \varphi_j^a(\mathbf{r}') V_c(|\mathbf{r}-\mathbf{r}'|) \varphi_k^b(\mathbf{r}') \varphi_l^b(\mathbf{r})$ and $\varphi_j^a(\mathbf{r})$ are the single-particle envelope wave functions on dot $j=L,R$ for conduction-band electrons ($a=e$) or holes ($a=h$). The tunneling matrix element T_e appearing in the exchange splitting \mathcal{J} is given by $T_e = t_e + V_{LL,LR}^{ee} \approx t_e + V_{RR,LR}^{ee} \lesssim 1$ meV and connects $|(1,1)S\rangle$ to $|(2,0)S\rangle$ and $|(0,2)S\rangle$. Here, t_e is the bare interdot electron tunneling matrix element.

Consider now a right-hand circularly polarized (σ_+) optical excitation with its optical axis along the heterostructure growth direction (z axis). This axis is defined with respect to the crystal axes of the quantum well structure on which the dots are grown, which typically defines the axis of shape asymmetry of the quantum dots (see Fig. 2). The light-matter interaction Hamiltonian in the dipole, rotating wave, and envelope function approximations is given by

$$V_+ = \frac{i\hbar}{2} \Omega_+ (\mathcal{M}_{RR} e_{R\downarrow}^\dagger h_{R\uparrow}^\dagger + \mathcal{M}_{LR} e_{L\downarrow}^\dagger h_{R\uparrow}^\dagger) e^{-i\omega_+ t} + \text{H.c.} \quad (1)$$

Here, $\Omega_+ \propto \frac{1}{2} \langle L^e=0, L_z^e=0 | x+iy | L^h=1, L_z^h=+1 \rangle$, where $|L^e=0, L_z^e=0\rangle$ is the periodic part of the conduction-band Bloch wave function which has s character, and $|L^h=1, L_z^h=+1\rangle$ is that of the valence-band electrons (or holes) which has p character, while \mathcal{M}_{RR} and \mathcal{M}_{LR} are the overlaps of the electron and hole envelope wave functions ${}_e\langle R | R \rangle_h$ and ${}_e\langle L | R \rangle_h$, respectively. The implicit assumption here is that the light-hole levels and the spin-orbit split-off hole band are energetically well separated from the heavy-hole band denoted by $|\uparrow\rangle = |J^h=3/2, J_z^h=3/2\rangle$, $|\downarrow\rangle = |J^h=3/2, J_z^h=-3/2\rangle$ ($J^h=L^h+S^h$) so that their optical coupling can be neglected, a well-justified approximation in zinc-blende (III-V) semiconductor quantum dots.¹³ Note that it is the correlation between the spin and spatial parts of the heavy-hole states ($|\uparrow\rangle = |L_z^h=1; \uparrow\rangle$, $|\downarrow\rangle = |L_z^h=-1; \downarrow\rangle$) which enables us to use selection rules based on pseudospin conservation. The excited-state

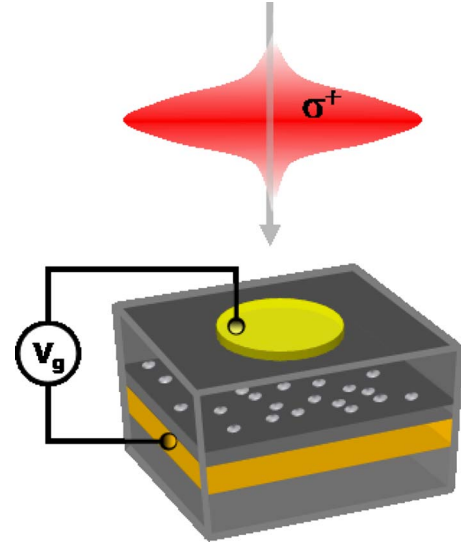


FIG. 2. (Color online) Schematics showing the optical excitation of the CQD system embedded in a Schottky-diode structure. The light pulse $\Omega_+(t)$ is incident along the crystal-growth direction (z axis).

manifold of doubly charged excitons (X^{2-}) is eight dimensional

$$|(2,1\uparrow)\sigma_h\rangle = e_{L\downarrow}^\dagger e_{L\downarrow}^\dagger e_{R\uparrow}^\dagger h_{R\sigma_h}^\dagger |0\rangle, \quad E_1 = E^{LLR},$$

$$|(2,1\downarrow)\sigma_h\rangle = e_{L\downarrow}^\dagger e_{L\downarrow}^\dagger e_{R\downarrow}^\dagger h_{R\sigma_h}^\dagger |0\rangle, \quad E_2 = E^{LLR},$$

$$|(1\uparrow,2)\sigma_h\rangle = e_{L\uparrow}^\dagger e_{R\uparrow}^\dagger e_{R\downarrow}^\dagger h_{R\sigma_h}^\dagger |0\rangle, \quad E_3 = E^{LRR} + \Delta,$$

$$|(1\downarrow,2)\sigma_h\rangle = e_{L\downarrow}^\dagger e_{R\uparrow}^\dagger e_{R\downarrow}^\dagger h_{R\sigma_h}^\dagger |0\rangle, \quad E_4 = E^{LRR} + \Delta,$$

where $\sigma_h = \uparrow, \downarrow$. We assume that because of the particular structure of the dots and the bias of choice, the optically generated hole always resides on the right dot within its lifetime. Here, $E^{LLR} = V_{LL,LL}^{ee} + 2V_{LL,RR}^{ee} - V_{LR,LR}^{ee} - 2V_{LL,RR}^{eh} - V_{RR,RR}^{eh}$, for instance, and $E^{LRR} > E^{LLR}$ because of the e - h attraction. An additional electron tunneling matrix element connects states $|(2,1\uparrow)\uparrow\rangle$ and $|(1\uparrow,2)\uparrow\rangle$ as well as $|(2,1\downarrow)\uparrow\rangle$ and $|(1\downarrow,2)\uparrow\rangle$, which gives rise to an anticrossing at around the bias $\Delta \approx E^{LLR} - E^{LRR} \approx 15$ – 20 meV. If we operate in the (1,1) regime (II) close to $V = V_1^*$ (Fig. 1), we can safely neglect any mixing of these X^{2-} states.

Consider the action of σ_+ optical excitation on the (1,1) ground-state manifold

$$V_+ |S\rangle = -\mathcal{M}_{RR} |(1\downarrow,2)\uparrow\rangle - \mathcal{M}_{LR} |(2,1\downarrow)\uparrow\rangle,$$

$$V_+ |T_0\rangle = -\mathcal{M}_{RR} |(1\downarrow,2)\uparrow\rangle + \mathcal{M}_{LR} |(2,1\downarrow)\uparrow\rangle,$$

$$V_+ |T_+\rangle = \mathcal{M}_{RR} |(1\uparrow,2)\uparrow\rangle - \mathcal{M}_{LR} |(2,1\uparrow)\uparrow\rangle,$$

$$V_+ |T_-\rangle = 0. \quad (2)$$

Here, we have discarded the common factor $(i\hbar/2)\Omega_+$. Note that there is no optical transition from $|T_-\rangle$ under σ_+ circular

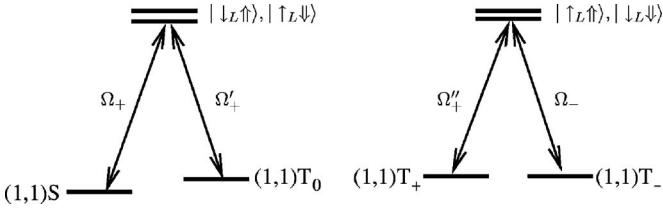


FIG. 3. Diagram showing the optical selection rules from the singlet-triplet ground state of the CQD to the intermediate excited states in a Raman spin-flip scheme. While $|(1,1)S\rangle$ and $|(1,1)T_0\rangle$ couple to the $|M|=1$ excited-state manifold, $|(1,1)T_+\rangle$ and $|(1,1)T_-\rangle$ couple to the $|M|=2$ subspace. Here, M refers to the spin projection of the total pseudospin of the left electron and the right hole.

polarization (and similarly, for σ_- and T_+). The following table illustrates the optical selection rules for transitions from $|(1,1)S\rangle$ and $|(1,1)T_0\rangle$ (Fig. 3).

	σ_+	σ_-	
\mathcal{M}_{RR}	$(1\downarrow, 2)\uparrow$	$(1\uparrow, 2)\downarrow$	E_1
\mathcal{M}_{LR}	$(2, 1\downarrow)\uparrow$	$(2, 1\uparrow)\downarrow$	E_3

Since $\mathcal{M}_{RR} \gg \mathcal{M}_{LR}$, the upper row transitions are strongest, while the lower row may be neglected.

The e - h exchange interaction in the relevant optically excited states would be negligibly small since the unpaired electron is exchange coupled to the hole that resides in a different dot. Starting with $|(1,1)S, T_0\rangle$, the states $|(1\downarrow, 2)\uparrow\rangle$ and $|(1\uparrow, 2)\downarrow\rangle$ will form the “bright” excitons X^{2-} , whereas the states $|(1\uparrow, 2)\uparrow\rangle$ and $|(1\downarrow, 2)\downarrow\rangle$ will form the bright excitons for the $|(1,1)T_\pm\rangle$ subspace.

Ideally, one would like to be able to connect all the members of the $(1,1)$ singlet-triplet space through a common optically excited state. In Eq. (2), however, the strong transitions under σ_+ circular polarization connect (S, T_0) and (T_+, T_-) to different excited states [$|(1\downarrow, 2)\uparrow\rangle$ and $|(1\uparrow, 2)\uparrow\rangle$, respectively]. One can envision manipulating the system with a combination of a static external magnetic field and optical fields to overcome this problem.

Consider applying an in-plane magnetic field $\mathbf{B} = B\hat{x}$. This will mix both the ground-state and the excited-state manifolds. Noting that the in-plane hole g factor is negligible, instead of rewriting the new states in the z representation, we will just rewrite the interaction Hamiltonian in the new electron spin-basis

$$V_+ = \frac{i\hbar}{2} \Omega_+ [\mathcal{M}_{RR}(e_{R\uparrow}^\dagger - e_{R\downarrow}^\dagger)h_{R\uparrow}^\dagger + \mathcal{M}_{LR}(e_{L\uparrow}^\dagger - e_{L\downarrow}^\dagger)h_{R\uparrow}^\dagger] e^{-i\omega_+ t} + \text{H.c.} \quad (3)$$

Here, $e_{L\uparrow}^\dagger$ now creates an electron with $S_x^e = +1/2$ ($|\uparrow_L\rangle$). The strong transitions now take the form

$$V_+|S\rangle = -\mathcal{M}_{RR}(|\uparrow_L\uparrow\rangle - |\downarrow_L\uparrow\rangle),$$

$$V_+|T_0\rangle = -\mathcal{M}_{RR}(|\uparrow_L\uparrow\rangle + |\downarrow_L\uparrow\rangle),$$

$$V_+|T_+\rangle = -\mathcal{M}_{RR}|\uparrow_L\uparrow\rangle,$$

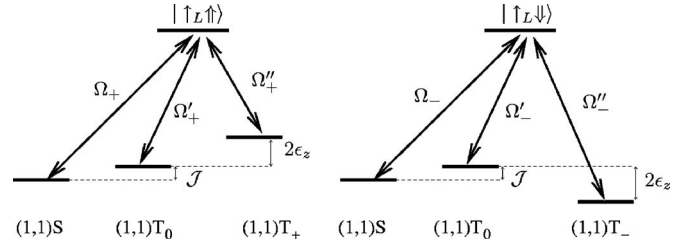


FIG. 4. Diagram showing the selection rules in the presence of an in-plane magnetic field. The previously derived selection rules for $B=0$ are no longer valid in this case, allowing for either $|T_+\rangle$ or $|T_-\rangle$ state to be coupled to the same intermediate state as that of $|T_0\rangle$ and $|S\rangle$. The two sets of ground-state manifolds can be accessed by using either left- or right-hand circularly polarized fields.

$$V_+|T_-\rangle = 0,$$

$$V_-|T_-\rangle = -\mathcal{M}_{RR}|\uparrow_L\downarrow\rangle.$$

Thus, one can couple either the submanifold (S, T_0, T_+) by σ_+ light to $|\uparrow_L\uparrow\rangle$ or (S, T_0, T_-) by σ_- to $|\uparrow_L\downarrow\rangle$ (we drop the explicit reference to the doubly-occupied orbital here). The excitation scheme for the circular polarization case is shown in Fig. 4.

Note that σ_+ polarized light couples $|(1,1)S\rangle$ and $|(1,1)T_0\rangle$ to $|\downarrow_L\uparrow\rangle$ as well. In this regard, it is important to have a Zeeman splitting ϵ_z ($\epsilon_z = g^e \mu_B B$ is the single electron Zeeman splitting) that is sufficiently large so that coupling of a single spin state to a single intermediate excited optical state may be possible.

Having an auxiliary state at disposal for optical manipulation is important in the implementation of robust qubit rotations based on STIRAP.¹⁴ The qubits in our CQD scheme above are formed by $(1,1)S$ and $(1,1)T_0$, which is a subspace that can be protected from hyperfine induced dephasing by spin-echo techniques.¹¹ Combined with the immunity to dephasing of the intermediate state that can be achieved by STIRAP, the above-described scheme seems to be well suited for generation and manipulation of qubit states for quantum information protocols in zinc-blende (III-V) semiconductor quantum dots.

III. OPTICAL MAPPING OF SPIN STATES

In this section, we discuss a scheme to efficiently prepare, manipulate, and map spin states of a doubly charged CQD into photon polarization for long-distance quantum state transfer.¹⁵

Consider the CQD system placed inside a high- Q cavity and the gate voltage tuned such that the system is in regime II, but close to the anticrossing at $V = V_1^*$. We furthermore apply an in-plane magnetic field. This will ensure that the states S , T_0 , and T_\pm are well separated in energy. Let us assume that the system is initialized to the superposition state

$$|\Psi\rangle = \alpha|S\rangle + \beta|T_0\rangle \quad (4)$$

in the qubit space composed of $(|S\rangle, |T_0\rangle)$. We first map this state into the state

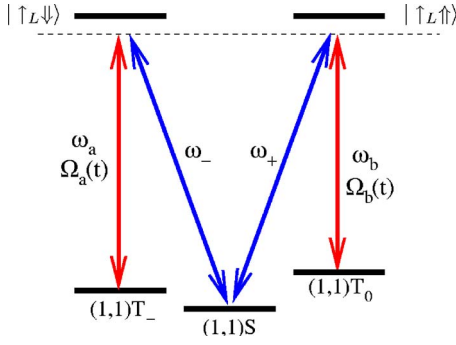


FIG. 5. (Color online) The cavity-assisted Raman scheme for spin-to-polarization mapping. The σ_- polarized laser at frequency ω_a and pulse shape $\Omega_a(t)$ results in cavity-assisted Raman transition to $|S\rangle$ when the two-photon resonance condition $\omega_- - \omega_a = E_{T_-} - E_S = \delta_1$ is satisfied. Similarly, the σ_+ polarized laser at frequency ω_b and pulse shape $\Omega_b(t)$ results in cavity-assisted Raman transition to $|S\rangle$ when $\omega_+ - \omega_b = E_{T_0} - E_S = \delta_2$. Note that the energy splitting between the excited states is negligible due to the small in-plane hole g factors.

$$|\Psi\rangle = \alpha|T_-\rangle + \beta|T_0\rangle \quad (5)$$

by a STIRAP sequence using σ_- polarized light as described, for example, in Ref. 16. The Raman nature of the scattering will ensure a robust state mapping.

We next turn on lasers with frequencies ω_a , ω_b , polarizations σ_- , σ_+ , and time-dependent Rabi frequencies $\Omega_a(t)$ and $\Omega_b(t)$, which are detuned by δ_1 and δ_2 from $|T_-\rangle - |\uparrow_L\downarrow\rangle$ and $|T_0\rangle - |\uparrow_L\uparrow\rangle$ transitions, respectively. The detunings δ_1 and δ_2 are carefully chosen so that the transitions $|\uparrow_L\downarrow\rangle - |S\rangle$ and $|\uparrow_L\uparrow\rangle - |S\rangle$ are resonant with a pair of degenerate cavity modes ω_- and ω_+ with orthogonal polarizations (see Fig. 5). Such cavities can be engineered using photonic band-gap structures where the cavity-mode splitting can be precisely tuned by atomic force microscopy oxidation so as to enforce the degeneracy condition required.¹⁷ The two-photon resonance condition for both polarizations will result in cavity-assisted Raman transition down to $|S\rangle$ and a transfer of the original spin state (4) to the polarization of the emitted single photon via

$$(\alpha|T_-\rangle + \beta|T_0\rangle)|0\rangle_{ph} \rightarrow |S\rangle(\alpha|1_{\sigma_-}\rangle_{ph} + \beta|1_{\sigma_+}\rangle_{ph}). \quad (6)$$

The resulting photons can then be used for long-range quantum communication in a distributed network of nodes containing CQD-cavity systems. For this to work reliably, we require the Purcell-enhanced decay rate to be faster than spin dephasing rates. Experimental parameters¹⁸ suggest this can be achieved by a factor of 100.

We now briefly discuss the potential practical difficulties for implementing these ideas in GaAs/InGaAs quantum dot systems. First, we remark that reliable creation of tunnel coupled double quantum dot systems has been established in experiment.^{6,7} Specifically, for strain-induced quantum dots, dots created in one layer will naturally create a strain field in a subsequent layer, leading to preferential formation of paired quantum dots with a distance well specified by the heterostructure growth process. Second, techniques for cou-

pling *pillars* of many quantum dots in a semiconductor membrane-based photonic crystal cavity have also been demonstrated,¹⁸ making the CQD-cavity systems a reasonable assumption for future devices. Finally, the quantum control techniques necessary for STIRAP and other such composite pulse sequences are well established, and, in principle, the speed and accuracy of these operations are limited only by the achievable laser power and stability.

IV. COHERENT OPTICAL MANIPULATION OF COUPLED QUANTUM DOTS WITH QUASIDEGENERATE VALENCE BANDS

We now show that coherent optical coupling between fine-structure states of doubly-charged double quantum dots could be achieved even when the intrinsic spin-orbit coupling of the semiconductor material is weak. We will rely on an external magnetic field and weak electron-hole symmetry breaking (differing electron and hole g factors) to show that all relevant Raman transitions are accessible.

Consider the possibility of optical manipulation of quantum dots where the spin-orbit effects are weak. The weakened selection rules result in the following optical interaction Hamiltonian

$$V_+ = \frac{i\hbar}{2}\Omega_+\mathcal{M}_{RR}\left(h_{R,3/2,3/2}^\dagger e_{R,1/2,-1/2}^\dagger + \frac{1}{\sqrt{3}}h_{R,3/2,1/2}^\dagger e_{R,1/2,1/2}^\dagger - \sqrt{\frac{2}{3}}h_{R,1/2,1/2}^\dagger e_{R,1/2,1/2}^\dagger\right)e^{-i\omega_+t} + \text{H.c.} \quad (7)$$

Here, h_{R,J_z}^\dagger creates a hole on the right dot with total angular momentum $\mathbf{J}^h = \mathbf{L}^h + \mathbf{S}^h$ and magnetic quantum number J_z , while $e_{R,1/2,\sigma}^\dagger$ creates an electron in the conduction band with spin projection $\sigma = \pm 1/2$. We only keep the strong, direct transition terms of the optical Hamiltonian. Considering now the action of σ_+ optical excitation on the (1, 1) ground-state manifold, we obtain

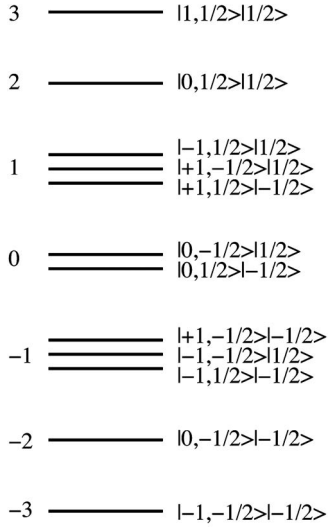
$$V_+|S\rangle = \mathcal{M}_{RR}\left[|(1\downarrow,2)3/2,3/2\rangle + \frac{1}{\sqrt{3}}|(1\uparrow,2)3/2,1/2\rangle - \sqrt{\frac{2}{3}}|(1\uparrow,2)1/2,1/2\rangle\right],$$

$$V_+|T_0\rangle = \mathcal{M}_{RR}\left[-|(1\downarrow,2)3/2,3/2\rangle + \frac{1}{\sqrt{3}}|(1\uparrow,2)3/2,1/2\rangle - \sqrt{\frac{2}{3}}|(1\uparrow,2)1/2,1/2\rangle\right],$$

$$V_+|T_+\rangle = -\mathcal{M}_{RR}|(1\uparrow,2)3/2,3/2\rangle,$$

$$V_+|T_-\rangle = \mathcal{M}_{RR}\left[\frac{1}{\sqrt{3}}|(1\downarrow,2)3/2,1/2\rangle - \sqrt{\frac{2}{3}}|(1\downarrow,2)1/2,1/2\rangle\right].$$

In principle, the degeneracy in the excited-state manifold presents a problem for coherent optical protocols due to po-



$$\langle f|V_+|T_0\rangle = 1/2,$$

$$\langle f|V_+|T_+\rangle = 0,$$

$$\langle f|V_+|T_-\rangle = 0.$$

However, if one is to consider a spin-flip Raman scattering from S to T_0 , there are two available paths via intermediate states $|f_1\rangle = |-1, \downarrow\rangle_h |\uparrow\rangle_e$ and $|f_2\rangle = |-1, \uparrow\rangle_h |\downarrow\rangle_e$. Only when the electron and hole g factors are different would these contributions allow a nonzero transition amplitude; otherwise, the two available paths will interfere destructively. Hence, it should, in principle, be possible to couple the states S, T_0 to each other via two-photon processes if the electron and hole g factors are different. In practice, the g factors should be sufficiently different to ensure $|\mu_B B_x (g^h - g^e)| > \gamma$, where γ is the broadening of the optically excited states.

FIG. 6. The energy-level structure of the excited-state manifold. On the left, the energies are given in units of $\mu_B B_x$. The additional smaller splittings are due to the possibly different g factors of electrons and holes, i.e., nonzero $\epsilon^{h,e}$. The states are written out explicitly in the format $|L_x^h, S_x^h|S_x^e\rangle$ where the electron spin refers to the left electron and the hole is on the right. The doubly occupied singlet electrons in the right quantum dot are not shown.

tential destructive quantum interference between different pathways. To overcome this difficulty, we consider the effect of a magnetic field. For simplicity, we assume a Voigt configuration ($\mathbf{B} = B\hat{x}$, say). The Zeeman Hamiltonian is given by

$$H_Z = \mu_B B_x (L_x^h + g^h S_x^h + g^e S_x^e), \quad (8)$$

where L_x^h and S_x^h are the x components of the hole orbital and spin angular momentum, respectively. Let us take $g^{h,e} = 2 + \epsilon^{h,e}$ with the hindsight that the spin-orbit interaction is weak. Then, one can easily see that the total angular momentum is not conserved. Thus, we have to use the $(L^h, L_x^h, S^h, S_x^h, S_x^e)$ basis. The energy-level structure is given in Fig. 6. In this basis, the optical interaction Hamiltonian is given by

$$V_+ = \frac{i\hbar}{2} \Omega_+ \mathcal{M}_{RR} (H_{\downarrow}^{\dagger} e_{R\uparrow}^{\dagger} + H_{\uparrow}^{\dagger} e_{R\downarrow}^{\dagger}) + \text{H.c.}, \quad (9)$$

where

$$H_{\sigma}^{\dagger} = \frac{1}{2} h_{R,-1,\sigma}^{\dagger} \sigma - \frac{1}{\sqrt{2}} h_{R,0,\sigma}^{\dagger} - \frac{1}{2} h_{R,+1,\sigma}^{\dagger} \sigma \quad \sigma = \uparrow, \downarrow. \quad (10)$$

The optical ground state is still given as above with the magnetic quantum numbers measured along x and with additional Zeeman energy contributions. The Zeeman contributions also split up the excited-state manifold, as shown in Fig. 6. Consider, for instance, the transitions to the final state $|f\rangle = |-1, \downarrow\rangle_h |\uparrow\rangle_e = e_{L\uparrow}^{\dagger} e_{R\downarrow}^{\dagger} e_{R\uparrow}^{\dagger} h_{R,-1,\downarrow}^{\dagger}$. We get $V_+ |S, T_0\rangle = V_+ (e_{L\uparrow}^{\dagger} e_{R\downarrow}^{\dagger} \pm e_{L\downarrow}^{\dagger} e_{R\uparrow}^{\dagger}) = e_{R\uparrow}^{\dagger} e_{R\downarrow}^{\dagger} (e_{L\uparrow}^{\dagger} H_{\uparrow}^{\dagger} \mp e_{L\downarrow}^{\dagger} H_{\uparrow}^{\dagger})$, which imply

$$\langle f|V_+|S\rangle = 1/2,$$

V. CONCLUSION

We have presented a scheme for optical manipulation of the metastable singlet-triplet subspace of a doubly charged CQD. We find that with strong as well as weak spin-orbit interactions, it is possible to implement Raman spin-flip transitions between a singlet and a triplet fine-structure-split ground state. Such Raman transitions enable the implementation of arbitrary coherent rotations robustly via quantum optical techniques previously proposed for single atoms or ions.

A key issue is the identification of the conditions that need to be satisfied in order to generate a spin-flip Raman scattering within a singlet-triplet space. In the absence of spin-orbit coupling and a degenerate p -like valence band, the optical Hamiltonian is a spin-0 operator. Thus, unless the spin-conservation law is broken in the intermediate state, it will not be possible to flip S to T_0 . In the strong spin-orbit case, the optical interaction Hamiltonian, however, is a reducible spin operator with nonzero projections on spin-1 and spin-0 subspaces (where spin is actually a pseudospin due to the restriction to the heavy-hole band). This particular property makes it possible to optically connect S and T_0 .

We expect that our findings will stimulate experimental research aimed at combining electrical and optical manipulations of confined spin states. The fact that optical manipulation is possible even for quantum dot structures with weak spin-orbit interaction enhances the prospects for pursuing experimental realization in a larger variety of solid-state systems.

ACKNOWLEDGMENTS

H.E.T. would like to thank Mete Atatüre, Jan Dreiser, and Alex Högele for useful discussions. J.M.T. would like to thank the Quantum Photonics group at ETH for their hospitality during his visit. J.M.T. acknowledges support from the Pappalardo Foundation. This work is supported by the Swiss National Research Foundation through the ‘‘Quantum Photonics NCCR.’’

- ¹*Semiconductor Spintronics and Quantum Computation*, edited by D. D. Awschalom, N. Samarth, and D. Loss (Springer-Verlag, Berlin, 2002).
- ²P. Michler, A. Kiraz, C. Becher, W. V. Schoenfeld, P. M. Petroff, L. D. Zhang, E. Hu, and A. Imamoglu, *Science* **290**, 2282 (2000).
- ³M. Pelton, C. Santori, J. Vuckovic, B. Y. Zhang, G. S. Solomon, J. Plant, and Y. Yamamoto, *Phys. Rev. Lett.* **89**, 233602 (2002).
- ⁴A. Imamoglu, *Fortschr. Phys.* **48**, 987 (2000).
- ⁵P. C. Haljan, P. J. Lee, K.-A. Brickman, M. Acton, L. Deslauriers, and C. Monroe, *Phys. Rev. A* **72**, 062316 (2005).
- ⁶H. J. Krenner, M. Sabathil, E. C. Clark, A. Kress, D. Schuh, M. Bichler, G. Abstreiter, and J. J. Finley, *Phys. Rev. Lett.* **94**, 057402 (2005).
- ⁷E. A. Stinaff, M. Scheibner, A. S. Bracker, I. V. Ponomarev, V. L. Korenev, M. E. Ware, M. F. Doty, T. L. Reinecke, and D. Gammon, *Science* **311**, 636 (2006).
- ⁸L.-M. Duan and G.-C. Guo, *Phys. Rev. Lett.* **79**, 1953 (1997).
- ⁹P. Zanardi and M. Rasetti, *Phys. Rev. Lett.* **79**, 3306 (1997).
- ¹⁰D. A. Lidar, I. L. Chuang, and K. B. Whaley, *Phys. Rev. Lett.* **81**, 2594 (1998).
- ¹¹J. R. Petta, A. C. Johnson, J. M. Taylor, E. A. Laird, A. Yacoby, M. D. Lukin, C. M. Marcus, M. P. Hanson, and A. C. Gossard, *Science* **309**, 2180 (2005).
- ¹²P. Jarillo-Herrero, S. Sapmaz, C. Dekker, L. P. Kouwenhoven, and H. S. J. van der Zant, *Nature (London)* **429**, 389 (2004).
- ¹³T. B. Bahder, *Phys. Rev. B* **41**, 11992 (1990).
- ¹⁴Z. Kis and F. Renzoni, *Phys. Rev. A* **65**, 032318 (2002).
- ¹⁵J. I. Cirac, P. Zoller, H. J. Kimble, and H. Mabuchi, *Phys. Rev. Lett.* **78**, 3221 (1997).
- ¹⁶F. Renzoni and S. Stenholm, *Opt. Commun.* **189**, 69 (2001).
- ¹⁷K. Hennessy, C. Högerle, E. Hu, A. Badolato, and A. Imamoglu, *Appl. Phys. Lett.* **89**, 041118 (2006).
- ¹⁸A. Badolato, K. Hennessy, M. Atature, J. Dreiser, E. Hu, P. M. Petroff, and A. Imamoglu, *Science* **308**, 1158 (2005).